System for Locating Faults in Multiterminal Transmission Lines

M. A. Nabi[1], Karanam Deepak[2], S. Namitha Reddy[3], Y. Bhargavi[4], B. Pavani Bai[5], and S. Karunya[6]

[1]Assistant Professor, Department of Electrical & Electronics Engineering, GPullaiah College of Engineering and Technology, Kurnool, Andhra Pradesh, India.abdulnabieee@gpcet.ac.in
[2]Assistant Professor, Department of Electrical & Electronics Engineering, GPullaiah College of Engineering and Technology, Kurnool, Andhra Pradesh, India,chandradeepak214@gmail.com
[3]Btech Scholar, Department of Electrical & Electronics Engineering, GPullaiah College of Engineering and Technology, Kurnool, Andhra Pradesh, India,namithareddy24@gmail.
[4]Btech Scholar, Department of Electrical & Electronics Engineering, GPullaiah College of Engineering and Technology, Kurnool, Andhra Pradesh, India.bhargaviyalamakuri@gmail.com
[5]Btech Scholar, Department of Electrical & Electronics Engineering, GPullaiah College of Engineering and Technology, Kurnool, Andhra Pradesh, India. bondilipavani03@gmail.com
[6]Btech Scholar, Department of Electrical & Electronics Engineering, GPullaiah College of Engineering and Technology, Kurnool, Andhra Pradesh, India.singarikarunya@gmail.com

Abstract—In this project, the creation and application of computer-based fault detection methods for transmission lines with multiple terminals are discussed.These methods are part of a fault-finding system that precisely locates the fault site by using voltage and current signal measurements from smart electronic devices installed on transmission-line terminals. The transformer loading, connection type, and electrical characteristics are all data that the algorithms have access to. The power system components used by the fault-location techniques are likewise presented in this project's phase component models.

Corresponding Author: chandradeepak214@gmail.com

1. INTRODUCTION

Transmission lines, which connect generation facilities to clients, are divided into different voltage categories. Frequently, high-voltage transmission cables contain just two terminals. On the other hand, Lateral branches from sub transmission lines,may connect to access a locations besides the main circuit and converge at electrical distribution centers.
Maintenance personnel often spend more time determining the fault site when a permanent fault occurs in these lines since the line section where the fault occurred is not marked. So, when maintenance costs increase, system dependability could decrease.
The issue became more complex as a result of deregulation.Substations attached to line branches are frequently not owned by the transmission company, and the current andvoltage measurements were taken at these substations, which could aid in problem detection, are not allowed to share with the transmission company for commercial reasons.

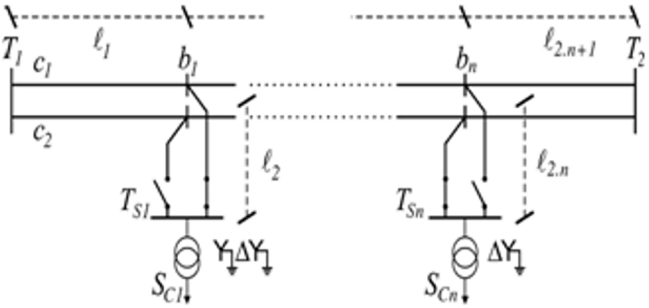

Fig.1. Multi-connectiontransmission network

A. Power transmission system

It is possible to use one, two, or more circuit lines in multiterminal transmission networks. Hence, the main conductor could be served bya single power line or dual-circuit power line. Figure 1 depicts an illustration of a multiterminal transmission network. Two terminals are connected by the main branch ($T_1$and T_2). Tap points ($b_1$to b_n) on a main branch allow lateral branches to be attached. These lateral branches culminate at substations for either industrial or distribution purposes (endpoints $T_{S1}$to T_{S2}).
It is the duty of the IEDs located at T_1 and T_2 to record voltage and current signals. It's possible that other terminals won't be able to access these records ($T_{S1}$to T_{S2}). However, the suggested method can precisely locate the breakdown area utilizing only the signals recorded at $T_1$and T_2, with or without temporal synchronisation. Additionally, the suggested approach makes use of the data, if they are available at other terminals, to support the validity of the conclusions.
As the recommended system can accurately estimate the load associated with each terminal, it may proceed with the issue location even if voltage and current data are unavailable at one or more of those terminals ($T_{S1}$to T_{S2}). It is important to note that transformers can be connected to these terminals via a grounded-wye, grounded star-delta, or grounded star system. Therefore, for failures that affect the ground, a significant finding portion of the fault current may flowthrough the transformer's primary winding. The current flowing in the primary winding must be implicitly accounted for in the mathematical equation used to represent the transformers due to the complexities of this scenario and the likely absence of voltage and current records at these terminals.

B. Fault-LocationMethods

For the purpose of locating faults in three terminal transmission lines, numerous suggested methods [1]– [6] have been made. Unfortunately, due to the problem's complexity, only a few alternatives for fault detection in multiterminal transmission lines have been reported[7]– [10]. The requirements listed in Part II aren't entirely addressed by these algorithms either.

In references [7] and [8] provide descriptions of methods for identifying faults in transmission lines with several terminals and a single circuit. These algorithms are based on the short transmission-linemodel and synchronized voltage and current measurements at all terminals. These algorithms may not properly handle medium or long multiterminal transmission lines due to accuracy issues.

Techniques for locating faults on transmission lines with multiple terminals and double circuits are described in references [9] and [10]. Both systems may have accuracy issues.when dealing with long and medium multiconnection transmission lines that rely on measurements of current and voltage at all terminals, as well as the short line transmission model. The first technique shows two distinct strategies employing synchronizedcurrent and voltage phasor values across contact points. It's uncertain whether the second one relies on time synchronization because it was developed using some odd, challenging assumptions.

These characteristics make the primary goal of the fault-finding method presented in this study to address every problem already raised in order to give a precise answer for fault finding in multi-terminal transmission lines solution for fault location.

2. MODELLING SYSTEM

This project's suggested fault-location approach is based on the phase components of current and voltage. It was important to create exact mathematical models for transformers, loads, and transmission lines in order to increase the correctness of the results. These models are discussed in the sections that follow.

A. TransmissionLine

In Fig. 2, A single-circuit power line of length $x$were represented by three-phase pi-model. Transmission line shunt admittance and series impedance matrices are $[z_{abc}]$and $[y_{abc}]$, respectively, per unit length. The mathematical relationship between the two phasors is current and voltage at the local and remote ends is seen in equation (1).

$$\begin{bmatrix} V_{abc}^{L} \\ I_{abc}^{L} \end{bmatrix} = [T_{(x)}] \times \begin{bmatrix} V_{abc}^{R} \\ I_{abc}^{R} \end{bmatrix} \text{and} \begin{bmatrix} V_{abc}^{R} \\ I_{abc}^{R} \end{bmatrix} = [T_{(x)}]^{-1} \times \begin{bmatrix} V_{abc}^{L} \\ I_{abc}^{L} \end{bmatrix} \quad (1)$$

Where

$$[T_{(x)}] = \begin{bmatrix} [A_{(x)}] & [B_{(x)}] \\ [C_{(x)}] & [D_{(x)}] \end{bmatrix} (2)$$

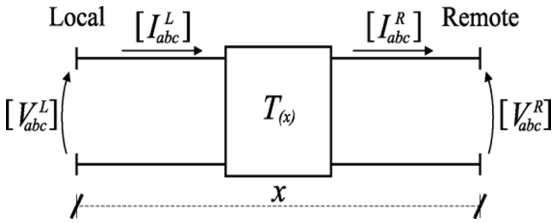

Fig.2.Pimodel line segment

And,accordingto[11]

$$[A_{(x)}] = [y_{abc}]^{-1} \times [M] \times \{[\cosh(\gamma_j \cdot x)]\} \times [M]^{-1} \times \quad [y_{abc}]$$

$$[B_{(x)}] = [y_{abc}]^{-1} \times [M] \times \{\gamma_j \cdot [\sinh(\gamma_j \cdot x)]\} \times [M]^{-1}$$

$$[C_{(x)}] = x \cdot [M] \times \left\{\left[\frac{\sinh(\gamma_j \cdot x)}{(\gamma_j \cdot x)}\right]\right\} \times [M]^{-1} \times [y_{abc}]$$

$$[D_{(x)}] = [M] \times \{[\cosh(\gamma_j \cdot x)]\} \times [M]^{-1}$$

Where

$[M]$eigenvectors of$[P] = [y_{abc}] \times [z_{abc}]$
γ_j^2eigenvectors of $[P]$
{[ ]}rectangular matrix method.
Calculating the parameters of single and double-circuit power transmission lines is feasible (3). The electromagnetic coupling is implicitly taken into account in the equations for double-circuit lines ($[z_{abc}]$ and $[y_{abc}]$ matrices are 6x6), and each line segment for transposed lines is described by a distinct $[z_{abc}]$ and $[y_{abc}]$ matrix.

B. Combination of Three-Phase Transformer and Load

The load can be modelled using fixed delta-connected impedances, and it is considered to be balanced, according to the load model. It's important to keep in mind that the suggested fault-location strategy is flexible enough to work with any other load situation. Moreover, no sizable production facilities are operating concurrently with this demand. Or to put it another way, the fault current is independent of the load. The connecting patterns of the transformer windings and the potentialpositive, negative and zero sequence network designs establish the phase component models of the transformers [12]. Hence, the load and transformer combination may be determined using admittance sequence matrices.

Consider, for instance, Fig. 3. Is the sequence network diagram.These schematics display a three-phase grounded-star/delta/ground-star transformercoupled to the load model that was previously explained. The combination's resulting admittance matrix is shown in Equation (4).

$$[I_{012}] = \begin{bmatrix} Y_0^C & 0 & 0 \\ 0 & Y_1^C & 0 \\ 0 & 0 & Y_2^C \end{bmatrix} \times [V_{012}] = [Y_{012}^C] \times [V_{012}] \qquad (4)$$

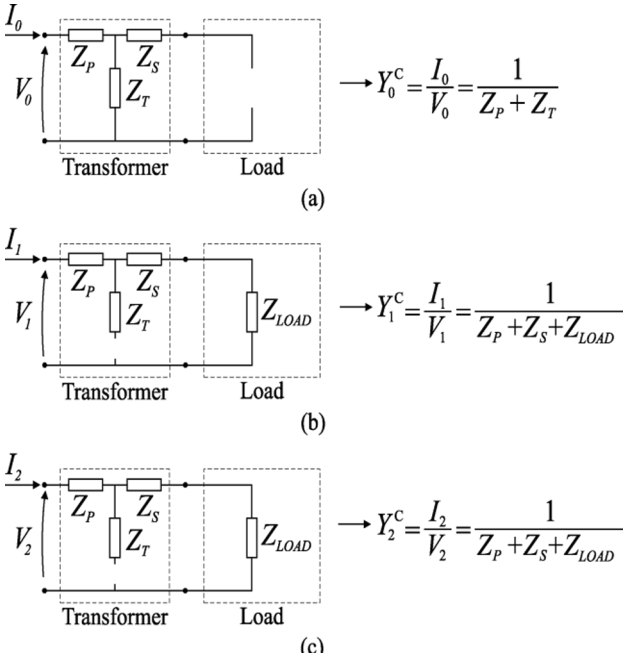

Fig.3.(a) positive sequence (b) negative sequence (c) zero sequence of load and transformer sequence network

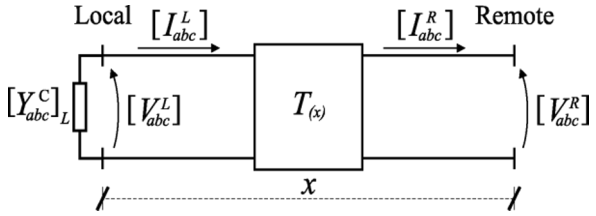

Fig.4. estimate the line section of $[Y_{abc}^{eq}]_x$

Also, by utilising (5) and (6) and the transformation matrix $[A]$, thephase elements of the current and voltage phasors can be determined.

$$[V_{012}] = [A] \times [V_{abc}] (5)$$

$$[I_{012}] = [A] \times [I_{abc}] \quad (6)$$

As a result, (4) evolves to

$$[I_{abc}] = [A]^{-1} \times [Y_{012}^C] \times [A] \times [V_{abc}] = [Y_{abc}^C] \times [V_{abc}] (7)$$

C. Combination of the Line Section, Load, and Converter

The suggested system also uses an equivalent matrix, which shows the load, line section, and transformer together, besides the admittance matrix, which specifies the combination of load and transformer. The tap points values of the voltage and current phasor were compared mathematically to construct this matrix.

Figure 4 shows a line segment with two endpoints (local and remote) separating it. The phasors of the current and voltage at the distant endpoints are obtained from (1) using the line length$x$ as the starting point, as in

$$\begin{bmatrix} V_{abc}^{R} \\ -I_{abc}^{R} \end{bmatrix} = \begin{bmatrix} [A_{(x)}] & [B_{(x)}] \\ [C_{(x)}] & [D_{(x)}] \end{bmatrix} \times \begin{bmatrix} V_{abc}^{L} \\ -I_{abc}^{L} \end{bmatrix} \quad (8)$$

Rewriting (7)

$$[-I_{abc}^{L}] = [Y_{abc}^{C}]_{L} \times [V_{abc}^{L}] \quad (9)$$

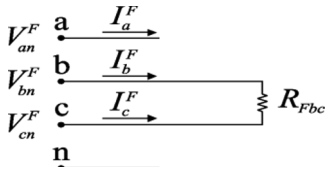

Fig.5. Fault in double power line (BC)

Plugging (9) in equation (8)

$$[V_{abc}^{L}] = \{[A_{(x)}] + [B_{(x)}] \times [Y_{abc}^{C}]_{L}\}^{-1} \times [V_{abc}^{L}] \quad (10)$$

The second system equation (8) yields the following when (9) and (10) are substituted (11). This equation explains the relation of the current and voltage phasor values at distantend mathematically.

$$[-I_{abc}^{R}] = [Y_{abc}^{eq}] \times [V_{abc}^{R}] \quad (11)$$

Where

$$[Y_{abc}^{eq}]_{x} = \{[C_{(x)}] + [D_{(x)}] \times [Y_{abc}^{C}]_{L}\} \times \{[A_{(x)}] + [B_{(x)}] \times [Y_{abc}^{C}]_{L}\}^{-1} \quad (12)$$

D. FaultModels

The fault type and component phases of the fault models are interdependent. All fault types and phases can be mathematically characterizedutilizing a relationship between the properties of the current and voltage phasor at the fault point, as in

$$[I_{abc}^{F}] = \left[Y_{abc}^{fault}\right] \times [V_{abc}^{F}] \tag{13}$$

Where

$\left[Y_{abc}^{fault}\right]$matrix of fault admittance;

$[V_{abc}^{F}]$values of the voltage phasor at the fault point;

$[I_{abc}^{F}]$phasor quantities at fault current.

The fault admittance matrix that accurately represents the mathematical correlation between voltage and current for all phases and types of faults can be generated in multiple ways. In the case of the double-line fault depicted in Fig. 5, a specific fault admittance matrix has been determined and is readily available.

$$\left[Y_{abc}^{fault}\right] = \begin{bmatrix} 0 & 0 & 0 \\ 0 & R_{Fbc}^{-1} & -R_{Fbc}^{-1} \\ 0 & -R_{Fbc}^{-1} & R_{Fbc}^{-1} \end{bmatrix} \tag{14}$$

3. SYSTEM FOR FAULT FINDING

The method fault-finding described in the research satisfies each of the requirements specified in Part II. Fault site detection is dependedon four steps, which were explainedclearly in the following sections.
Think of the network in Fig. 6 as an illustration of the suggested system. This network is made up of segments of single-circuit transmission wires. The primary branch, which connects the terminals T_1 and T_2, has three tap sites where lateral branches can be connected.

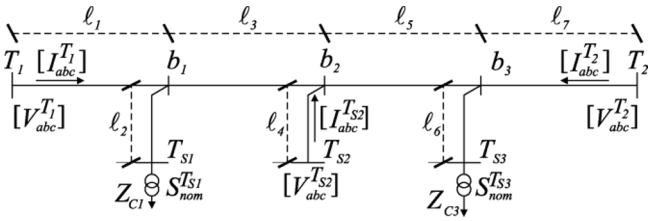

Fig.6.Transmissionnetwork.

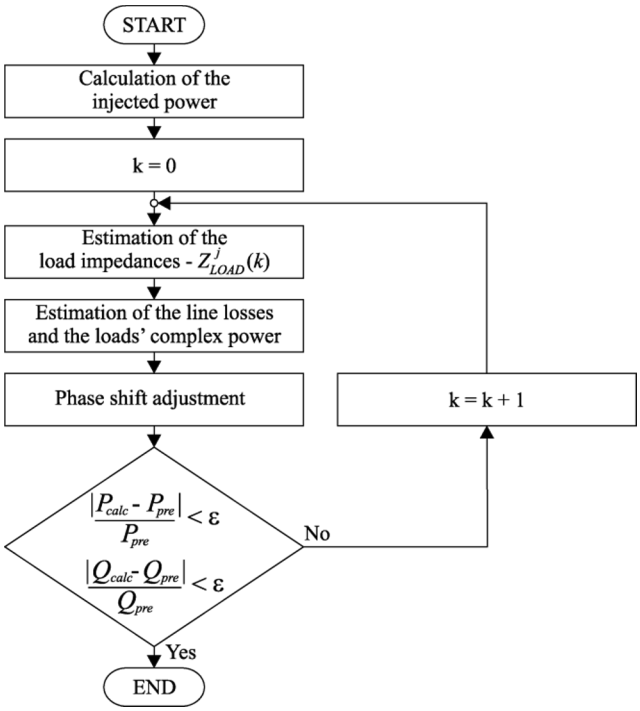

Fig.7.Prefaultprocessing.

The endpoints of these lateral branches areT_{S1}, T_{S2} andT_{S3}. The relative phases of these observations are uncertain because unsynchronized current and voltage measurements are only available at terminals T_1, T_2,andT_{S2}.

D. DigitalSignal Processing

Filtering before and after the fault current and voltage signals at terminals T_1, T_2, and T_{S2}reduces the influence of the fault's exponential components[13]. The pre and post fault voltage values as well as the current phasor values at the associated endpoints are thendetermined using the distinct Fourier transform method with one cycle.

E. Prefault Data Processing

The current and voltage phasor values at endpoints T_1, T_2, and T_{S2} are synchronised during the prefault processing stageandestimates the load impedances at the other terminals using a recursive approach ($T_{S1}$and T_{S3}).

This strategy, which is depend upon five phases discussed in sections III-B1 through III-B5, is seen in Fig. 7.

1) Calculating the power injected:

The current and voltage phasor values at endpoints T_1, T_2, and T_{S2} are used to calculate the reactive and active prefault injected power ($P_{pre}$and Q_{pre}) at the reference terminal (such as T_1) in the algorithm's initial step. The computed injected power is equal to the sum of losses in line plus power load consumption at endpoints $T_{S1}$and T_{S3}.

2) Initial Estimate of the Load Impedances:

Using the assumption that the transformers linked to terminals T_{S1} and T_{S3} function proportionately to their nominal apparent power, the algorithm predicts the inceptive value of load impedances at these endpoints after computing the injected power.

$$P_c^j = P_{pre}\frac{s_n^j}{\sum_{j=T_{S1};T_{S3}} s_n^j} \text{and} Q_c^j = Q_{pre}\frac{s_n^j}{\sum_{j=T_{S1};T_{S3}} s_n^j} \quad (15)$$

$$Z_c^j = \frac{3\left(V_n^j\right)^2}{\left(P_c^j + j\cdot Q_c^j\right)^*} \quad (16)$$

Where

$T_j T_{S1}$ and T_{S3};
S_n^j Apparent power of Transformer nominal at Terminal T_j;
P_c^j Power is Active at terminal T_j;
Q_c^j Power is Reactive at terminal T_j;
Z_c^j Initial estimation of terminal T_j load impedance;
V_n^j Voltage of Nominal phase at terminal T_j.

3) Calculating the Complex Power of line losses and loads:

To analyze the system, the load impedances at terminals T_{S1} and T_{S3}, as well as the phasors of voltage and current at terminals $T_1, T_2,$ and T_{S2} are taken into consideration. By utilizing the phasor values of current and voltage at the reference terminal T_1, it is possible to determine the voltage and phasor quantities at the tap points b_1, and also calculate the losses that occur along the line section between T_1 and b_1.

Moreover, the load complex power at T_{S1} and the losses of the line segment $b_1 - T_{S1}$ may be calculated using the voltage phasor values at b_1(11). By using this method, the complex power of all loads and losses of all line sections may be estimated (P_{calc} and Q_{calc}).

4) Phase-Shift Adjustment:

By utilizing the measurements of voltage and current phasors at endpoint T_1, along with estimated load impedances at endpoints T_{S1} and T_{S3}, the method described in the preceding section allows for the calculation of current and voltage phasor quantities at terminals T_2 and T_{S3}.As an outcome, by contrasting the phasor values of voltage and current measured and calculated at these endpoints T_2 and T_{S2}, as shown in [7] and [14], the phase shift of with respect to T_1 and it can be estimated.

5) Load impedances of estimation:

Initial estimations of the load impedances may not be accurate. It must be rectified in addition of loads of the complex power and the losses in line to the total injected power. The impedance loadis changed in each iteration.

$$Y_c^j(k+1) = Re\{Y_c^j(k)\}\cdot\frac{P_{pre}}{P_{calc}} + j\cdot Im\{Y_c^j(k)\}\cdot\frac{Q_{pre}}{Q_{calc}} \quad (17)$$

Where

$Y_c^j(k+1)$ terminal load admittance of T_j;
k Number of iteration

F. Processing of postfault:

During the post-fault processing stage, two sets of post-fault current and voltage phasor values are determined for all tap locations. One set uses terminals T_1 and T_2 to obtainpost-fault voltage and current phasor values, while the other set utilizes only terminal T_1 . On (1) and (2), this stage is built (11). It is dependent on the post-fault voltage and current phasor values at terminal T_{S2} ,theimpedance of load at endpoints T_{S1} and T_{S3} , and terminal T_{S2} impedances. Aspart of the computations, it also assumes that the system is not flawed.

With this technique, it is possible to determine whether the issue was with the primary branch or any lateral branches. Along those lines:

- In the case of a fault occurrence on a lateral branch, it is necessary for the post-fault voltage phasor values obtained from both sets at the relevant tap point to be equal.
- If not, it is necessary to verify each segment of the line that is connected to the main branch, where the issue was. Here, the fault-detection system can only examine the pertinent feeder branch.

To estimate the position of the fault, two algorithms were created. The postfault voltage and current phasor amounts at both ends are the foundation of the first one (Section III-D). There are two methods used to identify faults on line segments from the main branch or twigs. The initial approach involves utilizing voltage and phasor quantities that are accessible at the relevant substation terminals. In contrast, the second approach relies on examining the post-fault current and voltage phasors at one end and is utilized to identify problems occurring in lateral branches where only the current and voltage phasor values are obtainable at the tap point.

G. Using current and voltage at Fault-Findingmethodology

When the phasor quantities of voltage and current are available at both terminals of a line section, the fault-location algorithm proposed in this section, as suggested in [15], is utilized to locate faults.

As an illustration, let us consider the line section that is portrayed in Fig. 8, which forms a constituent part of the system that is exhibited in Fig. 6. The fault site is situated at an unknown distance $x$from the tap pointsb_1, which define the boundaries of the line section, and its length is denoted by l_3. In this case, it is possible to determine the post-fault current and voltage phasor quantities at terminals T_1 andT_2 by utilizing equations (1) and (11), respectively, and the post-fault current and voltage phasor values measured at those terminals.

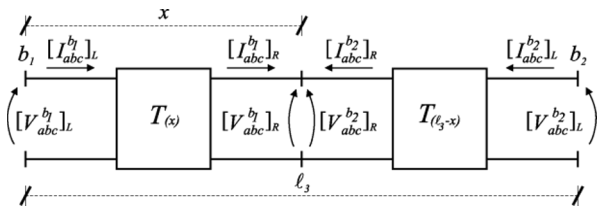

Fig.8.Linesection T_1 and T_2

As a result, the postfault current and voltage phasor quantities at the fault spot can be estimated.

$$\begin{bmatrix} V_{abc}^{b_1} \\ I_{abc}^{b_1} \end{bmatrix}_R = \begin{bmatrix} [A_{(x)}] & -[B_{(x)}] \\ -[C_{(x)}] & [D_{(x)}] \end{bmatrix} \times \begin{bmatrix} V_{abc}^{b_1} \\ I_{abc}^{b_1} \end{bmatrix}_L \quad (18)$$

$$\begin{bmatrix} V_{abc}^{b_2} \\ I_{abc}^{b_2} \end{bmatrix} = \begin{bmatrix} [A_{(l_3-x)}] & -[B_{(l_3-x)}] \\ -[C_{(l_3-x)}] & [D_{(l_3-x)}] \end{bmatrix} \times \begin{bmatrix} V_{abc}^{b_2} \\ I_{abc}^{b_2} \end{bmatrix}_L \quad (19)$$

To calculate the fault distance, it is essential to compare the voltage phasor measurements at the location of the fault, which can be obtained from equation (18) with the corresponding phasor quantities calculated using equation (19). This comparison is crucial because it allows for an accurate assessment of the fault location.

$$[\Delta V_{abc}^{fault}] = [A_{(x)}] \times [V_{abc}^{b_l}]_L - [B_{(x)}] \times [I_{abc}^{b1}]_L - [A_{(l_3-x)}] \times [V_{abc}^{b_2}]_L + [B_{(l_3-x)}] \times [I_{abc}^{b_2}]_L \quad (20)$$

The suggested algorithm solves (20) using the same golden section search technique as in [16]. The fault distance is unaffected by the fault resistance, or the source impedances since this technique solely considers the variation of voltage phasor values at fault location.

E. One-End Current and Voltage Fault-Location Algorithm

When current and voltage phasor values are only known at one end of a line segment, the algorithm presented in this section is utilized to find defects there.
Fig. 9's line section, which is a component of the system shown in Fig. 6 as an illustration, is one such case.The fault location is still situated at an unknown distance x from the tap point b_1 that defines this line section. Terminal T_{S2}, which is placed at the end of this linesection, has a length of l_2. By utilizing equations (1) and (11), it is possible to determine the post-fault current and voltage phasor quantities at terminals T_1 and T_2, based on the post-fault current and voltage phasor values that are obtainable at b_1. Similar to the prior method, the assumption is made that the fault is a simple series fault, which facilitates the calculation of the post-fault current and voltage phasor values at the fault location.

$$\begin{bmatrix} V_{abc}^{b_1} \\ I_{abc}^{b_1} \end{bmatrix}_R = \begin{bmatrix} [A_{(x)}] & -[B_{(x)}] \\ -[C_{(x)}] & [D_{(x)}] \end{bmatrix} \times \begin{bmatrix} V_{abc}^{b_1} \\ I_{abc}^{b_1} \end{bmatrix}_L \quad (21$$

$$[I_{abc}^{fault}] = [I_{abc}^{b_1}]_R \times [I_{abc}^{TS1}]_R = [Y_{abc}^{fault}] \times [V_{abc}^{b_1}]_R \quad (22)$$

Where

$$-[I_{abc}^{T_{S1}}]_R = [Y_{abc}^{eq}]_{(l_2-x)} \times [V_{abc}^{b_1}]_R \quad (23)$$

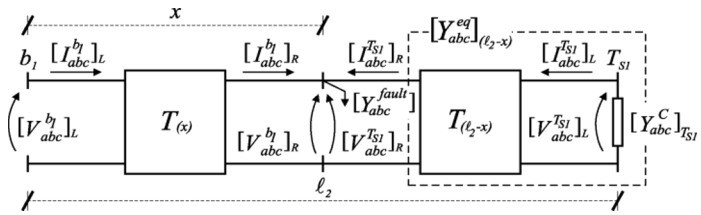

Fig.9. Line section T_1 and T_{S1}

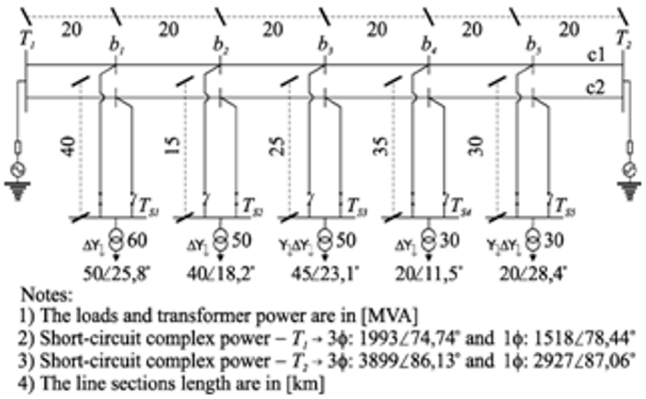

Notes:
1) The loads and transformer power are in [MVA]
2) Short-circuit complex power – $T_1 \rightarrow 3\phi$: 1993∠74,74° and 1ϕ: 1518∠78,44°
3) Short-circuit complex power – $T_2 \rightarrow 3\phi$: 3899∠86,13° and 1ϕ: 2927∠87,06°
4) The line sections length are in [km]

Fig.10. network of simulation

replacing (23) inequation (22)

$$\left([Y^{fault}_{abc}] + [Y^{eq}_{abc}]_{(l_2-x)}\right) \times [V^{b_1}_{abc}]_R = [I^{b_1}_{abc}]_R \quad (24)$$

To ascertain the location of the fault accurately, it is imperative to employ the current and voltage phasor values that are available at the tap point b_1. Bysubstituting equation (21) with equation (24), it is feasible to establish a connection between these phasor values and the admittance fault matrix, as well as the equivalencematrix $[Z_{eq}]$, in the following manner:

$$[V^{b_1}_{abc}]_L - [Z_{eq}] \times [I^{b_1}_{abc}]_L = [0] \quad (25)$$

Where

$$[Z_{eq}] = \left\{[A_{(x)}] + [B_{(x)}] \times \left([Y^{fault}_{abc}] + [Y^{eq}_{abc}]_{(l_2-x)}\right)\right\} \times \left\{[C_{(x)}] + [D_{(x)}] \times \left([Y^{fault}_{abc}] + [Y^{eq}_{abc}]_{(l_2-x)}\right)\right\}^{-1} \quad (26)$$

The equivalent impedance matrix$[Z_{eq}]$solely depends on the distance and the components of the fault admittance matrix because the loads' impedance was calculated during the prefault data processing step, as in

$$[Z_{eq}] = f(x, [Y_{abc}^{fault}]) \quad (27)$$

The equivalent impedance matrix's components and distance $\boldsymbol{x}$estimates are what make up the fault-location methodology (25). It states that there are multiple equivalent impedance matrices that need to be considered due to the various types of faults and phases involved, and that the fault-location technique utilizes the Newton-Raphson approach to estimate the performance of this task (25).

Think of a phase A-related line-to-ground fault as an illustration. The fault distance $\boldsymbol{x}$ and the component of the fault admittance matrix form the equivalent impedance matrix, as shown in

$$[Z_{eq}] = f(x, Y_{Fa}) \quad (28)$$

The proposed method starts with a first guess for each variable to estimate x and Y_{Fa} before continuing with a recursive procedure in which these values are updated each time, as in

$$x(k+1) = x(k) + \Delta x(k) \quad (29)$$

$$Y_{Fa}(k+1) = Y_{Fa}(k) + \Delta Y_{Fa}(k) \quad (30)$$

Where k is the number of iterations, and $\Delta x(k)$ and$\Delta Y_{Fa}(k)$can be obtained through problem solving.

$$[V_{abc}]_L - [Z_{eq}]_{(k)} \times [I_{abc}]_L$$

$$= [\Delta V_{abc}^{b_1}]_k$$

$$= \left\{ \frac{\partial [Z_{eq}]_{(k)}}{\partial x} \Delta x(k) + \frac{\partial [Z_{eq}]_{(k)}}{\partial Y_{Fa}} \Delta Y_{Fa}(k) \right\} \times [I_{abc}]_L \quad (31)$$

The system must be solved using a fitting data technique since there are more equations than variables. The least-squares approach is used in the algorithm this study proposes, and it is described in [14].

F. Determine the line section of fault

Two probable fault sites are identified using the fault-location method suggested in this study. One of the positions is located at the feeder branch, which is often overlooked and not well documented, while the other position is situated on a significant section of the main branch. This information is based on Section III-C. It is of little consequence thar each line section's fault distance and function value are provided by the examination of the main branch (as stated in equation 20). The function value at the malfunctioning line segment should be equal to 0 in the event that a fault develops on the main branch. By considering each component, only one viable option can be either the main branch or the lateral branch based on the calculated fault distance and function value for each line section.

4. SIMULATION RESULTS

G. Sub-transmission network

ATP test data was used to simulate the fault-location system. Fig. 10 depicts the topology of the subtransmission network employed in various simulations. The nominal voltage of this network, which connects terminals $T_1$and T_2, is 138 [kV]. It consists of a main branch with two circuits. Five tap points along the main branch are used to join parallel branches. These branches come to a conclusion at the distribution substations $T_{S1}$to T_{S5}.

In the simulated situations, the tower and conductors were representative of voltage level 138 $[kV]$, as shown in Fig.11.This line segment, consisting of 266.8 ATP line constants, were simulated using the ATP line constants supporting approach.

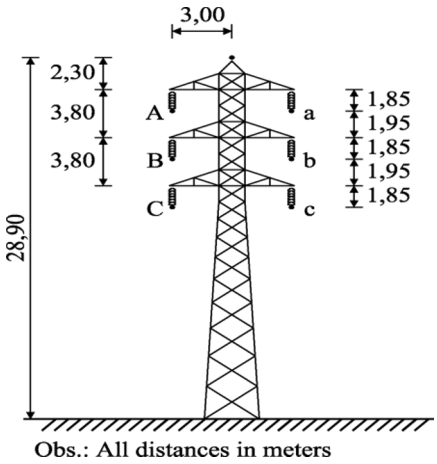

Fig.11. Simulation in Electric tower

TABLE 1
Computational Results

Fault type	Fault instant [ms]	Number of points	R_F [Ω]	Number of simulations
AN	33.33 37.50	22	0, 1, 5, 20, 50, 100	264
BC BCN	33.33	22	0, 1, 5	132
ABC	33.33	22	0, 1	44

MCM ACSR phase conductors, a ground wire 1/2 high-strength steel (HS), and midspan sag of 6.5 meters.

The fault parameters presented in Table I were used for ATP simulations. The simulations involved four types of faults, which were conducted at 22 different locations. The fault resistances used in the simulations ranged from 0 to 100 ohms[Ω]. In accordance with the power of the loads shown in Fig. 10, the loads are modelled as constant impedances. 440 simulated cases were created as a consequence.

The correctness of the system was tested using the simulated examples given in Table I, and such outcomes are shown in Segments IV-B through IV-D.

H. Current and voltage values were measured at all Terminals

The fault-detection system findings are reported in this section since measurements of current and voltage are available at all line terminals.
The fault location distance errors for line-to-ground, double-line, double-line-to-ground, with three-phase faults are shown in Table II for fault resistances ranging from 0 to 50[Ω]. As said, for all fault types, the actual faults are less than 440 [m]. When three-phase, double-line-to-ground, and double-line faults are taken into account, the mean errors are comparable. Yet, compared to other faults, line-to-ground faults have a significantly larger means inaccuracy (111 [m]). Nonetheless, when compared to the length of the line, these inaccuracies are quite little.

I. Measurements of current and voltage were taken at terminals T_1 and T_2.

The results of the fault-location system presented in this section are based on the assumption that only measurements of voltage and current at endpointsT_1 and T_2 are available.

TABLE II
At all terminals, fault location results and measurements were obtained.

Fault type	error [m] min	max	mean	Standard deviation [m]
AN	0	432	111	96
BC	3	248	93	80
BCN	1	246	80	72
ABC	1	288	52	48

TABLE III
At terminals $T_1$and T_2, fault location results and measurements were obtained

Fault type	error [m] min	max	mean	Standard deviation [m]
Algorithm described in section IV-D				
AN	1	585	168	128
BC	0	44	18	12
BCN	0	52	19	16
ABC	0	132	38	37
Algorithm described in section IV-E				
AN	1	1708	290	379
BC	84	1029	305	260
BCN	78	1042	290	271
ABC	1	848	175	248

It is evident from Table III that the accuracy of fault location is influenced by the fault type and resistance (ranging from 0 to 50[Ω]). Notably, two distinct fault location techniques were assessed and compared in Sections III-D and III-E. Specifically, the approach outlined in section III-E yielded superior results for line-to-ground faults with distances of under1710$[m]$, double-line faults with distances of under 1050$[m]$, and double-line-to-ground faults with distances of under900$[m]$. The first algorithm's response exhibits a better level of accuracy, as can be shown. This is because the second fault-location algorithm's accuracy may be hampered by the precision of the estimates of the loads'

impedances. Even still, both methods' faults are quite insignificant as compared to the line length.

J. Resistance of fault influence

Several line-to-ground failures with fault resistances ranging from 0 to 100 [Ω] were simulated in order to examine the impact of the fault resistance. Table IV shows the mistakes related to fault distance location.

This table shows that, when all fault resistances were taken into account, the method described in segment III-D provided faultsless than 1000 $[m]$. On the other hand, for fault resistances up to 50 [Ω] and for 100 [Ω], these describe the method in Section III-E producederrors less than 1710$[m]$ and less than 3070$[m]$, respectively. This is owing to the fact that, for lesser fault currents, the loads' impedances may considerably affect how accurately the fault-location algorithm operates.

The efficiency of the strategy suggested in Section III-D is affected by the fault resistance, as shown in Fig. 12. The behaviour of the function given by (20) at the faulty line segment is shown in this figure for fault resistances ranging from 0 to 100[Ω].

The impedance values for the loads used in the simulations were used to create Fig. 12(a), whereas Fig (b)

TABLE IV
Fault Resistance influence

Fault type	**error [m]**			**Standard deviation [m]**
	min	**max**	**mean**	
Algorithm described in section IV-D				
0	12	223	113	67
1	10	223	114	68
5	1	233	119	73
20	16	349	180	104
50	23	585	315	168
100	17	932	527	288
Algorithm described in section IV-E				
0	6	810	143	232
1	3	825	147	238
5	22	884	196	248
20	3	1148	327	323
50	1	1708	639	539
100	233	3063	1558	990

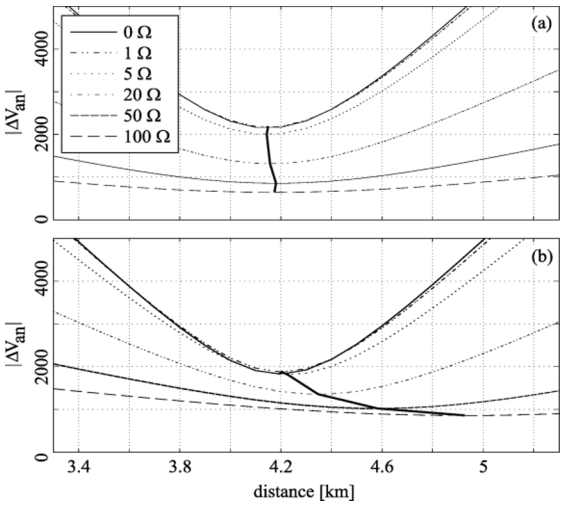

Fig. 12.Result of function as stated by (20).

was obtained by utilizing the impedances of the predicted loads. In first scenario, the detection of fault is unaffected by the fault resistance; in certain terms, the average offunction remains constant across all fault impedance. The fault site shifts to the right in the second scenario, though. By comparing the two figures, it is feasible to state with certainty that the fault-location method did not cause this impact, but rather mistakes in the calculation of the loads' impedances.

5. CONCLUSION

A fault-location system for multiterminal transmission lines was developed, put into use, and its test results were described in this study. The algorithms that make up the proposed system were also discussed in depth.

The outcomes show that the accuracy of the algorithms is sufficient. The greatest inaccuracy of the method is almost below 1000 meters as well as 3100 meters, correspondingly (0.4% as well as 1.2% of the entire length of the line).

According to Section IV, the proposed system's correctness is dependent on the specifics of the models that the algorithms utilize as well as the data that is accessible at all line. The accuracy of the Section IV-B results was presented is higher compared to those in Section IV-C, due to the availability of voltage and current signals at the line terminals in the former, as opposed to only being available at T_1 and T_2 in the latter.

The calculation of the load impedances has an impact on the proposed fault-location system, as shown in Section IV-D, for fault resistances greater than $50[\Omega]$. The outcomes are still precise, though.

REFERENCES

[1] R.K.Aggarwal,D.V.Coury,A.T.Johns,andA.Kalam,"Apracticalapproachtoaccuratef aultlocationonextrahighvoltageteedfeeders,"*IEEETrans.PowerDel.*,vol. 8,no.3,pp.874–883,Jul.1993.

[2] A. Girgis, D. Hart, and W. Peterson, "A new fault location techniquefor two and three terminal lines," *IEEE Trans. Power Del.*, vol. 7, no.1,pp.98–107,Jan.1992.

[3] C. Yu, C. Liu, and Y. Lin, "A fault location algorithm for transmission lines with tapped leg—PMU based approach," in *Proc. IEEE Power Eng. Soc. Summer Meeting*, Vancouver, BC, Canada, 2001,pp.915–920.

[4] A. D. Tziouvaras, J. B. Roberts, and G. Benmouyal, "New multi-endedfaultlocationdesignfortwo-orthree-terminallines,"in*Proc.7thInst.Elect.Eng.,DevelopmentsinPowerSystemProtectionInt .Conf.*,Amsterdam, TheNetherlands, 2001,no.479, pp.395–398.

[5] Y. Lin, C. Liu, and C. Yu, "A new fault locator for three-terminal trans-mission lines using two-terminal synchronized voltage and current phasors,"*IEEETrans.PowerDel.*,vol.17,no.2,pp.452–459,Apr.2002.

[6] L.L.Lai, N.Rajkumar, E.Vaseekar, H.Subasinghe, A.Carter,andB. J.Gwyn, "Wavelet transform and neural networks for fault location of a teed-network," in *Proc. Int. Conf. Power System Technology*, Perth,Australia, Jul.2000,vol.2,pp. 807–811,PowerCon2000.

[7] M.Abe, N.Otsuzuki, T.Emura, and M.Takeuchi, "Development of a new fault location system for multi-terminal single transmission lines, "*IEEE Trans. Power Del.*, vol.10, no.1, pp.159–168,Jan.1995.

[8] S. M. Brahma, "Fault location scheme for a multi-terminal transmission line using synchronized voltage measurements," *IEEE Trans.PowerDel.*, vol.20,no. 2, pt. 2, pp.1325–1331,Apr. 2005.

[9] T. Nagasawa, M. Abe, N. Otsuzuki, T. Emura, Y. Jikihara, and M.Takeuchi, "Development of a new fault location algorithm for multi-terminal two-parallel transmission lines," *IEEE Trans. Power Del.*, vol.7,no.3,pp.1516–1532,Jul.1992.

[10] T. Funabashi, H. Otoguro, Y. Mizuma, L. Dube, and A. Ametani, "Digital fault location for parallel double-circuit multi-terminal transmission lines, "*IEEETrans .Power Del.*, vol.15,no.2,pp.531–537,Apr.2000.

[11] W. I. Bowman and J. M. McNamee, "Development of equivalent Piand T matrix circuits for long untransposed transmission lines," *IEEETrans. Power App. Syst.*, vol. PAS-83, no. 6, pp. 625–632, Jun. 1964,653-657.

[12] D. S. Ramos and E. M. Dias*, Sistemaselétricos de potência—Regimepermanente*, G. Dios, Ed.Rio de Janeiro, Brazil: Ed. GuanabaraDois,1983,vol.2.

[13] N. N. de Santana, "Pré-filtragem da component eaperiódic a exponencial paraos algoritmos utilized osemrelés digitaisd edistância," M.Sc. dissertation, Escola Politécnicada USP, SãoPaulo,Brazil,1998.

[14] G. Manassero, Jr., "Sistema Para localização de faltasemlinhas de transmissã ocomsu bestaçõesconectadasemderivação,"Ph.D.dissertation,Escola Politécnica daUSP, São Paulo,Brazil,2006.

[15] A. T. Johns and S. Jamali, "Accurate fault location technique for powertransmission lines," *Proc. Inst. Elect. Eng., Gen., Transm. Distrib.*, vol.137,no.6,pt.C,pp.395–402,Nov.1990.

[16] W. H. Press, S. A. Teukolsky, W. T. Vetterling, and B. P. Flannery, *Numerical Recipes in C*. Cambridge, MA: Cambridge Univ. Press, 1992.